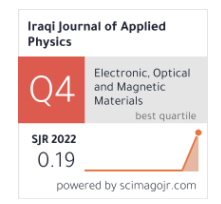
Roaa J. Mohammed Jassim M. Mansoor Nabeel K. Hussein

Department of Physics, College of Science, University of Diyala, Diyala, IRAQ



Influence of Multi-Layered CdO Thin Films on Their Ability to Detect Toxic Gases

This research investigates the influence of a number of coated layers on the gassensing properties of cadmium oxide (CdO) thin films prepared using the spin coating technique on glass substrates. Structural examinations, including X-ray diffraction (XRD), revealed a consistent cubic polycrystalline nature. Atomic Force Microscopy (AFM) elevated roughness and grain sizes with increased layering. Scanning Electron Microscopy (SEM) showcased a cauliflower-like morphology on the films. The optical band gap also narrowed marginally from 2.65 eV (2-layer) to 2.53 eV (5-layer). Hall effect studies confirmed n-type conductivity, with enhanced mobility. Gas sensing assessments identified the 5-layer CdO film, termed CD-4, as highly responsive to H₂S, achieving 72% sensitivity at 200°C and a swift 14-second response. This work elucidates CdO film gas-sensing dynamics, emphasizing layer optimization's significance.

Keywords: Sol-gel; Cadmium oxide; Surface Morphology; Gas sensing **Received:** 30 November; **Revised:** 10 January; **Accepted:** 17 January 2024

1. Introduction

Cadmium oxide (CdO) is a well-recognized metal-oxide-semiconductor (MOS) material with ntype conductivity. It is characterized by a narrow band gap, often within the 2.2 to 2.7 eV range [1]. The electrical resistivity of this material is often found to be within the range 10^{-2} - 10^{-4} Ω .cm, a characteristic that may be ascribed to imperfections such as oxygen vacancies and cadmium interstitials [2]. Additionally, it should be noted that CdO exhibits a very high level of optical transmission within the visible region of the solar spectrum, with a measured rate of around 90%. Also, CdO thin films exhibit remarkable electrical conductivity. As a result, it offers significant promise for several applications, such as flat panel displays, organic light-emitting diodes, and gas sensors. CdO nanostructures have been fabricated using several processes, including the sol-gel approach [3], hydrothermal [4], solvothermal deposition [5], chemical bath deposition [6], pulsed-laser deposition [7], spray pyrolysis [8], and sputtering deposition [9,10]. The sol-gel spin coating process is notable among this set of technologies for its simplicity, costeffectiveness, and little need for advanced film consolidation and preparation equipment. This methodology facilitates the creation of films characterized by exceptional homogeneity and meticulous regulation of their content [11].

The presence of crystallinity significantly impacts the electrical properties of semiconductors, which in turn forms the base for gas sensitivity. There have been several reports on the use of CdO semiconductors in gas sensors to detect diverse gases. The duration required for recovery is often in the range of tens of seconds when exposed to high temperatures; however, at room temperature (RT), it often extends to several minutes. Achieving high efficiency in gas sensing at room temperature is a much sought-after objective due to the adverse effects

of greater operating temperatures on energy consumption. This, in turn, has implications for the mobility and safety of explosive gas detection systems [12].

Hydrogen sulfide (H₂S) gas was strictly selected as the testing gas in this study for several compelling reasons. Primarily, H2S is a highly toxic and hazardous gas commonly produced in industrial settings, such as heavy water treatment plants for nuclear reactors, crude petroleum extraction, natural gas processing, and through the biological decomposition of organic waste material. Its presence in these environments poses significant health risks, including potential damage to the human cardiovascular, respiratory, and nervous systems. Exposure to H₂S gas concentrations above 300 ppm can be particularly dangerous, leading to sudden cardiovascular collapse and severe damage to the lungs and nervous system. Given these hazards, developing sensitive and selective H₂S gas sensors is crucial for human safety [13].

The gas sensing mechanism depends on the reaction with the surface of the metal oxide layer, mainly by the presence of oxygen ions adsorbed on the surface. This interaction leads to a modification in the concentration of charge carriers within the material. A change in the charge carriers' concentration modifies a material's electrical conductivity (or resistance). A predominance of electrons characterizes an n-type semiconductor as the primary charge carrier, and its conductivity is enhanced when exposed to a reducing gas. On the contrary, the presence of an oxidizing gas reduces charge-carrying electrons inside the sensor layer, causing a decline in conductivity [14]. The gassensing characteristics of metal oxide semiconductors are influenced by many aspects, including the operating temperature, shape, and

composition [15]. The operational temperature has a crucial role in gas sensitivity.

The objective of this study was to investigate the influence of different numbers of coated layers through spin coating on the morphological, electrical, and structural properties of CdO thin films produced via the sol-gel method. The ultimate goal was to achieve optimal characteristics for the gas-sensing properties of thin films consisting of CdO material, intending to advance the properties of thin films.

2. Experimental Part

The deposition of cadmium oxide (CdO) films onto glass substrates was carried out by a sol-gel spin coating technique using SPER spin concrete instrument (L2001A3-E461-UK). Chemicals with a purity of 99% were supplied from Scharlau Corporation. To prepare 0.5m CdO solutions, cadmium-acetate dehydrate (Cd(CH₃COO)₂,2H₂O) was dissolved in 2-methoxyethanol using magnetic stirring at 27 °C for 20 minutes. The temperature of the solution was gradually increased to 70 °C while stirring for 2 hours to achieve homogeneity, transparency, and colorlessness. Monoethanolamine (MEA) stabilizer was added to the solution to maintain a molar ratio of metal ions to MEA at 1:1. The ultimate solutions were allowed to cool down to ambient temperature, kept undisturbed for 24 hours, and thereafter subjected to filtration using a paper filter. Prior to the application of a coating, the sodalime glass (SLG) substrates underwent a cleaning process, including the use of acetone, ethanol, and water, which were applied by the method of sonication. The coating parameters used in this study were a rotational speed of 3300 rpm for 35 s. Following the application of a coating, the thin films underwent a drying process on a plate at a temperature of 200 °C for a duration of 15 minutes, to eliminate the solvent and any residual organic matter. The CdO films were produced by applying the appropriate number of coatings sequentially on the same glass substrate, followed by thermal treatment the film at a temperature of 475 °C for one hour. The aforementioned procedure was iterated to generate films with two, three, four, and five layers as symbol of CD-1, CD-2, CD-3, and CD-4, respectively.

The crystalline structure of CdO films was analyzed using an x-ray diffractometer (XRD Phillips X-Pert) with Cu-K α radiation (wavelength of 1.54 Å) within 20 range of 20°-80°. A cross-sectional analysis was performed using a Zeiss Sigma field-emission scanning electron microscope (FE-SEMS) and atomic force microscopy (AFM) using an advanced second-generation TT-2 microscope. The electrical properties of the film were determined through Hall measurements utilizing the Ecopia HMS-3000Ver 3.5 instrument from the USA. All measurements were conducted at room temperature, which was set at 27°C. For sensing measurements, a custom-built system was employed.

3. Results and Discussion

The x-ray diffraction (XRD) patterns of CdO films with varied numbers of layers (two, three, four, and five) were analyzed and characterized, as shown in Fig. (1). This was done so that the patterns could be compared and contrasted. The research showed that all of the different CdO film depositions have an identical cubic polycrystalline Significantly, the XRD patterns displayed welldefined peaks at precise 2θ angles of 33°, 38°, 55°, 66°, and 69°, which corresponded to the crystallographic planes (111), (200), (220), (311), and (222), respectively. The preferred orientation along (111) direction for all samples. This observation aligns closely with prior research findings [16-18] and is consistent with the criteria outlined in the ICDD reference (75-0592). Moreover, it was evident that the intensity of these peaks increased with a rise in the number of layers in the films, indicating an enhancement in crystallinity [18,19]. Furthermore, the determination of the lattice parameter "a" for all films resulted in a value which closely resembled the reported value of 4.6948 Å for CdO crystals in the ICDD database.

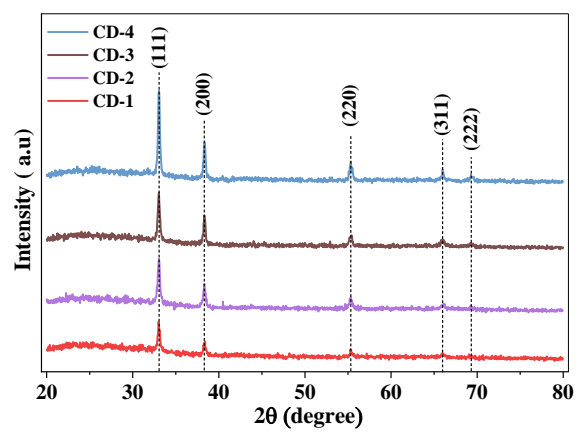


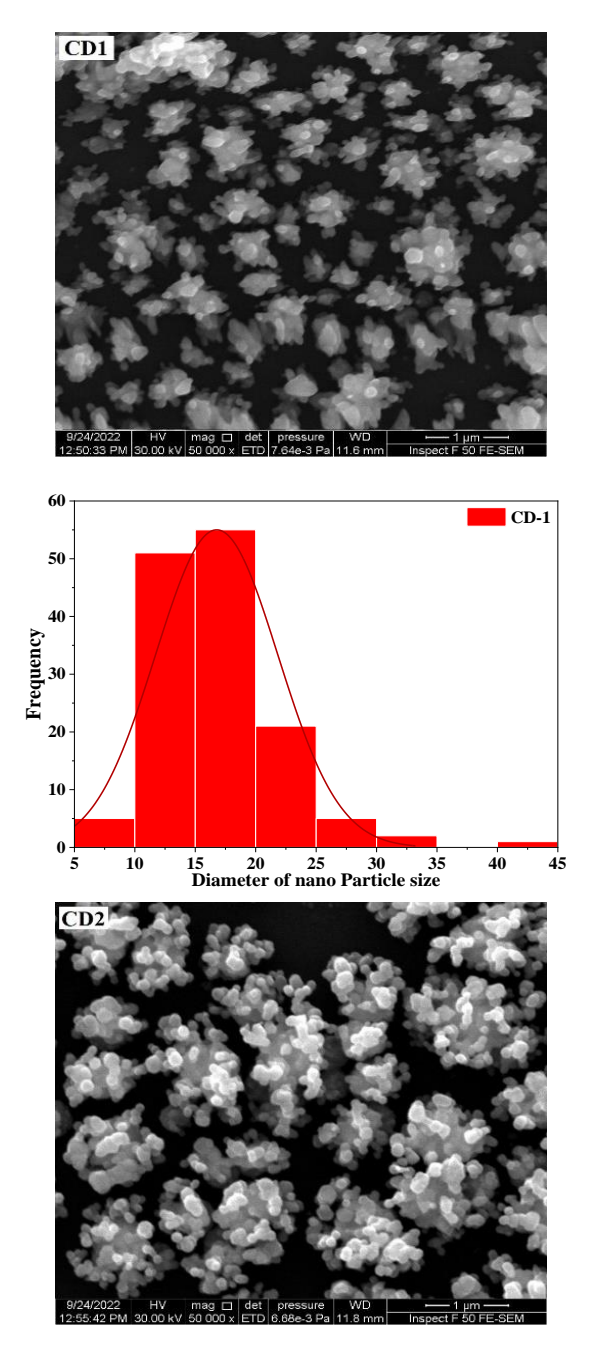
Fig. (1) The XRD patterns of CdO films with different layers

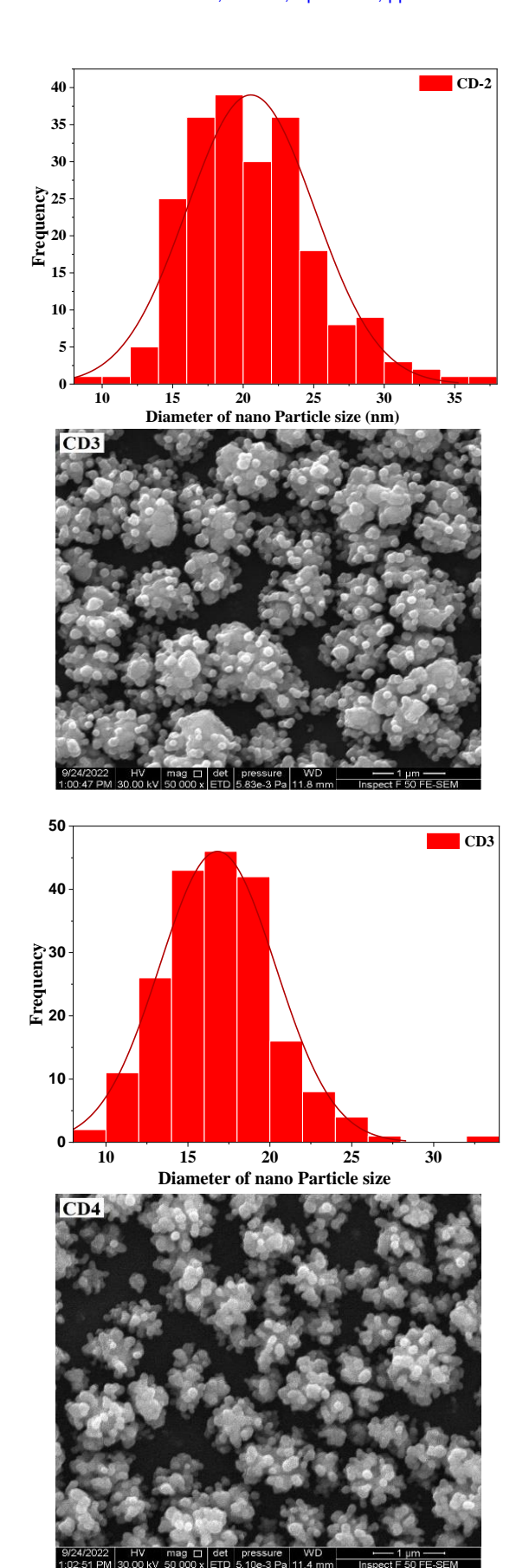
In the following equation, the variable k is a factor that relies on the relative alignment of the scattering vector with the external configuration of the crystallite. Additionally, λ denotes the wavelength, β represents the width of the XRD line, and θ corresponds to the diffraction angle measured from the position of Bragg's angle. It was observed that the dimensions of the crystallites experienced an increase from 23.4 to 29.7 nm as the number of layers in the investigated CdO thin films was increased [20]. The crystallites size (D) was estimated using Scherrer's relation [21]:

$$D = \frac{k\lambda}{\beta \cos\theta} \tag{1}$$

This discovery aligns with the results documented in a prior investigation. The determination of the average crystallite size associated with the most notable diffraction peaks has been conducted and is listed in table (1). Additionally, table (1) presents information on the angular positions of the diffraction peaks, the associated measurements of the full-width-at-half-maximum (FWHM), the inter-planar spacing (d_{hkl}) , and lattice constant (a) of successive crystalline planes, as determined using the diffraction angles (2θ) .

Figure (2) displays the top-view FE-SEM images at a magnification of 50 KX. These images depict the distinct layers of CdO thin films that were fabricated at ambient temperature utilizing the spin coating technique on glass slide substrates. The micrographs depict the presence of a cauliflower-like morphology on the surface of the CdO thin films, these results are consistent with [22].





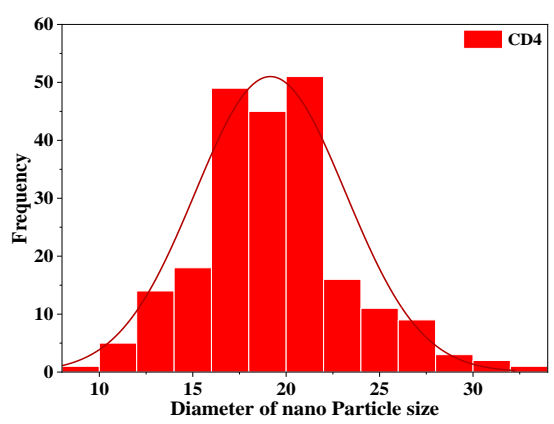
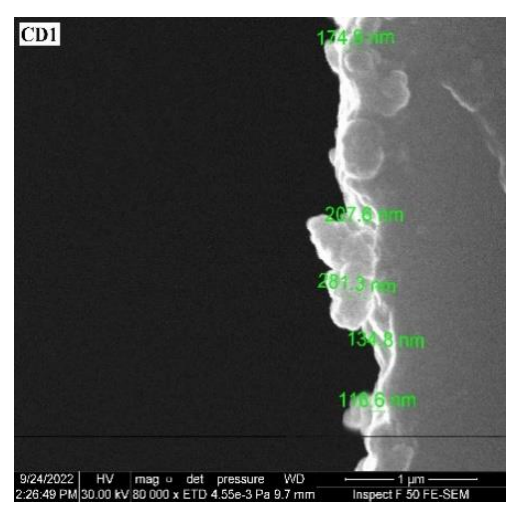


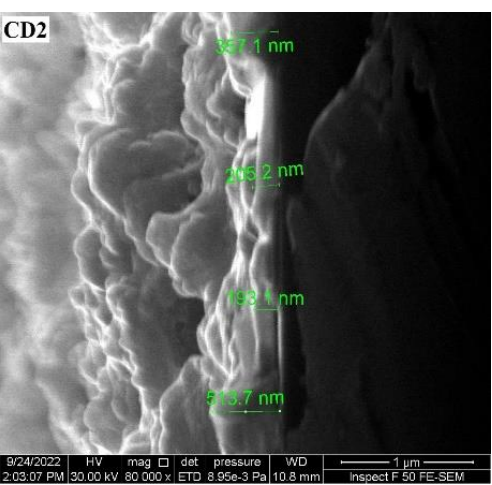
Fig. (2) FE-SEM images and cross-sectional distributions of CdO thin films prepared in this work

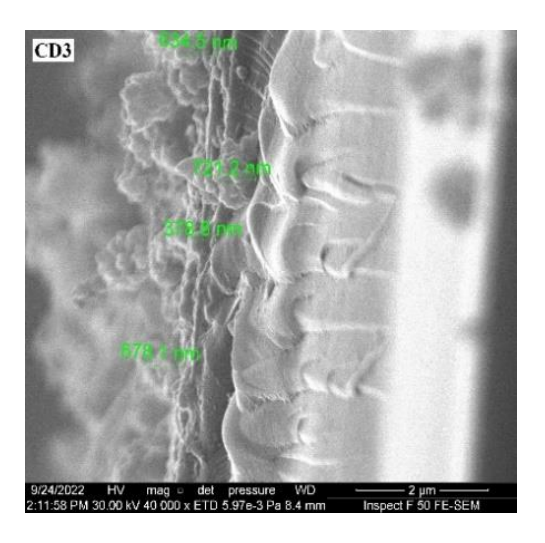
As the number of layers is increased, there is an observed alteration in both the surface morphology and particle size. More precisely, there is a decrease in the spatial separation between particle streams. The presence of a spherical nanocluster structure in CdO has been documented in prior studies. The surface roughness seen in the samples may be explained by the gradual rise in film thickness, which leads to an increase in volume and, subsequently, porosity. This discovery aligns with previous research findings and is substantiated by the microscopic pictures obtained from FE-SEM analysis. The observed correlation between porosity and thickness is consistent with the findings of the XRD results, which establishes a positive relationship between crystal size and the thickness of the sensing layer [23].

The thicknesses of the thin layers were quantified using tomographic analysis utilizing FE-SEM, and the corresponding findings are visually shown in Fig. (3). In contrast, a non-uniform augmentation in thickness was seen as the number of layers increased.

In order to quantitatively analyze the elements present, energy-dispersive x-ray spectroscopy (EDX) was employed. The fundamental principle underlying EDX operation involves the utilization of unique atomic emission spectra exhibited by each element in response to x-ray excitation. This allows for the differentiation and characterization of various elements based on their distinct spectra. Figure (4) illustrates the elemental composition of the substance based on the percentage distribution relative to their corresponding atomic weights. EDX confirmed the presence of Cd and O [24]. The specific concentration value of Cd in the CdO films can be found in Fig. (4).







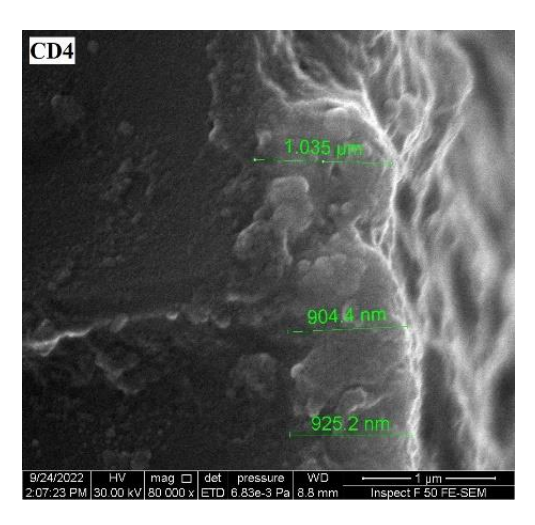


Fig. (3) Cross-sectional FE-SEM images for measuring the thickness of the deposited layers

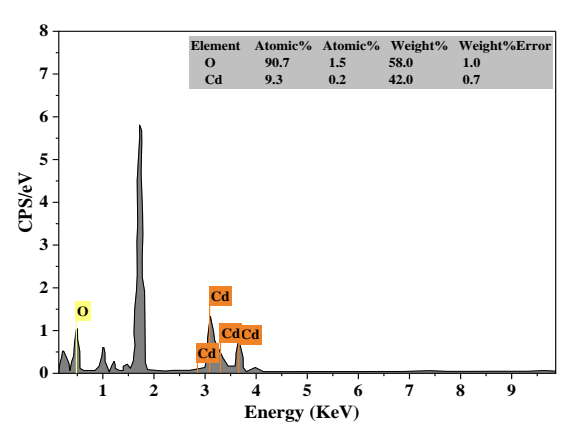
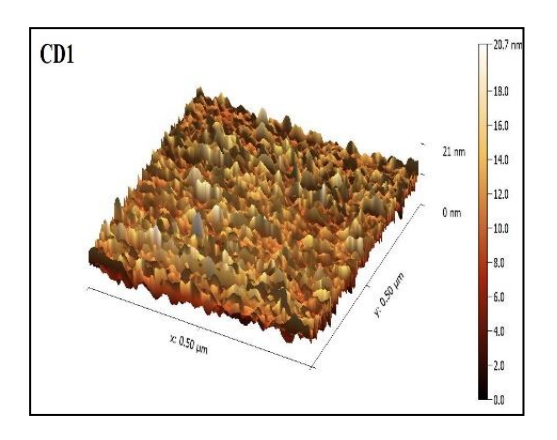
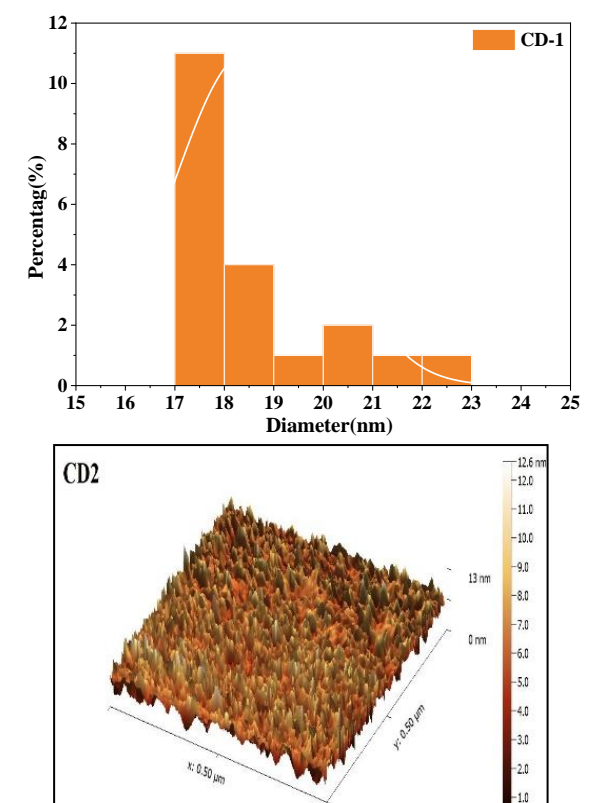
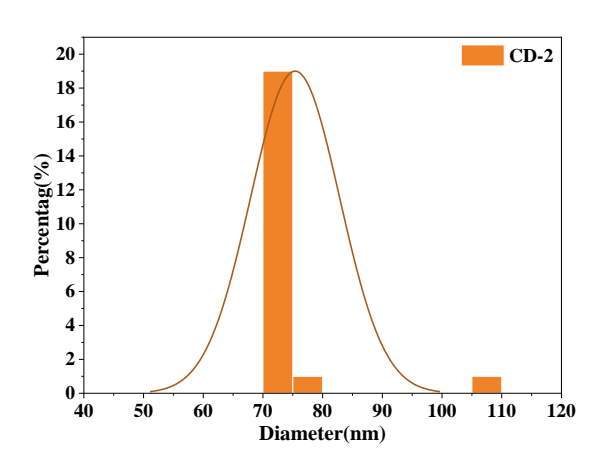


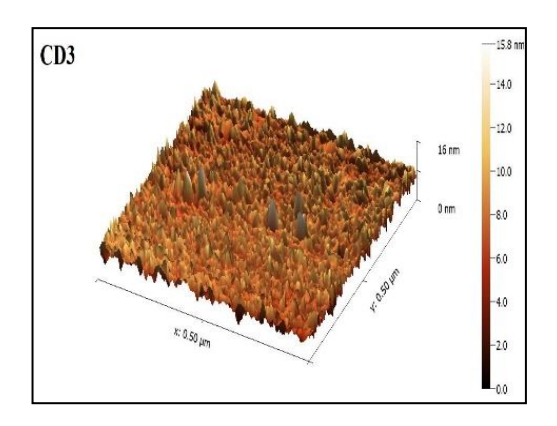
Fig. (4) EDX spectrum of CdO thin film

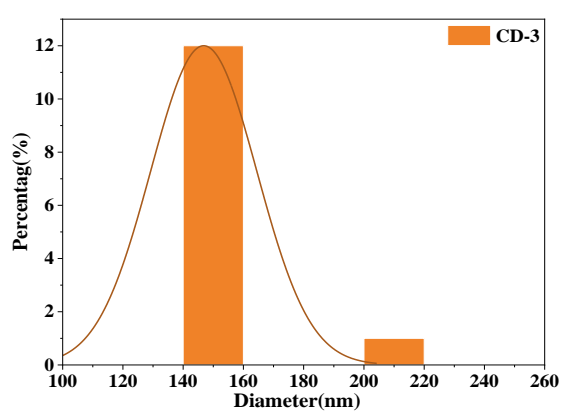
Figure (5) illustrates the three-dimensional (3D) AFM images and the accompanying cumulative histogram to illustrate the particle size distribution on the surface of CdO thin films deposited on glass substrates. The AFM images present significant observations that increasing in the number of layers results in a rising in roughness, root mean square (RMS) value, and grain size. These findings are consistent with the results obtained from the XRD analysis. The CdO thin films exhibited a diverse range of grain sizes, ranging from roughly 38.26 to 311.4 nm. It is particularly noted that the grain size distribution in samples CD-2 and CD-3 appears more consistent compared to other samples. The transition from a single-mode to a double-mode particle size distribution as the number of layers increases indicates the formation of cluster-like aggregations. This phenomenon is further supported by the cauliflower-like formations seen in the FE-SEM images. Furthermore, it was noticed that the film's surfaces were decorated with spherical particles of nanoscale dimensions.

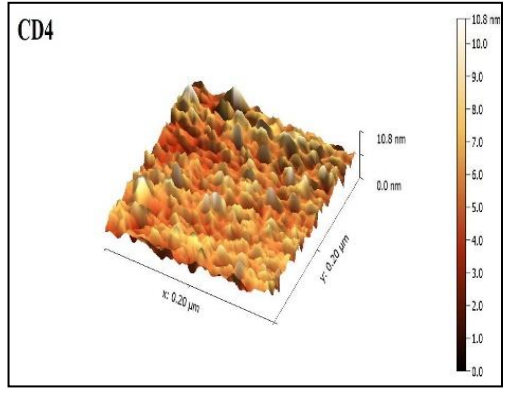












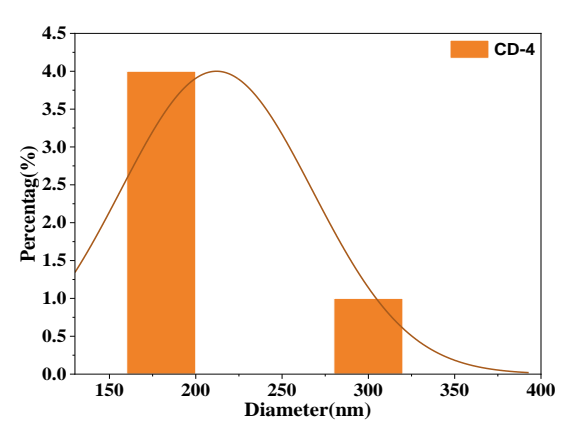


Fig. (5) 3D AFM images and size distributions for CdO films with different number of layers on a glass substrate

The increase in grain size, which includes a range of sizes, directly impacts the film's overall roughness. The roughness value of the film rises from 5.425 to 75.90 nm with increasing No of layers from 2 to 5

layers [25]. A substantial body of research provides evidence that materials with larger specific surface areas, which are frequently associated with increased roughness, provide improved gas-sensing capabilities [23].

To compute the absorption coefficient for the frequency associated with the highly absorbent region, equation (2) can be used. This involves using the values of absorbance (A) and thickness (t) to derive the coefficient.

$$\alpha = 2.303 \frac{A}{t} \tag{2}$$

The absorption spectra for the CdO films with different numbers of layers (two, three, four, and five) in the wavelength range of 300-900 nm are depicted in Fig. (6). This figure illustrates a clear trend wherein the absorbance of all samples falls as the wavelength increases.

The contribution to the electrical conduction process is attributed to photons whose energies are equivalent to or higher than the energy gap required to excite electron-hole couples. The aforementioned property has a prevailing presence in materials classified as semiconductors [26]. Furthermore, the red shift in the spectra, which becomes more pronounced with an increasing number of layers, is linked to an increase in crystalline size, as demonstrated by the XRD results. This increase in the size is likely to reduce the quantum confinement effect that is typical in nano-sized particles, consequently leading to a decrease in the energy gap. This change is what manifests as a red shift in the spectra [27]. Moreover, it has been shown that the absorption spectrum exhibits an upward trend as the number of layers rises, which can be attributed to the corresponding increase in sample thickness. These results are consistent with [18,19]. The absorption edges of the samples exhibit a progressive increase, suggesting a relatively limited level of crystallinity [28].

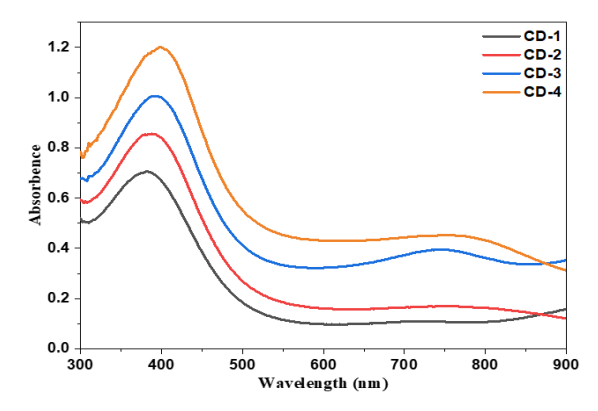


Fig. (6) UV-visible absorption spectra of CdO thin films

The calculation of the optical bandgap (E_g^{opt}) was performed for CdO films with different numbers of layers using the Tauc's formula, specifically Eq. (3). The determination of the optical bandgap values was achieved by plotting $(\alpha hv)^2$ versus the photon energy

(hv), as seen in Fig. (7). The intersection of the tangent of the curve with the x-axis was used to identify the optical bandgap values.

$$\alpha h \nu = B(h \nu - E_g)^r \tag{3}$$

The energy bandgap of all samples exhibits an increase compared to the established value for the bulk form, which may be attributed to the nano effect. A drop in the optical bandgap was seen, with the 2-layers sample exhibiting a value of 2.65 eV, while the 5-layers sample had a lower value of 2.53 eV. These results are consistent with previously published works [18,19]. The observed reduction in the optical bandgap may be ascribed to the crystal defects can be formed which produce localized states that change the defective Fermi level due to an increase in carrier concentrations [19]. Also, the decrease of direct band gap with the increase of thickness can be attributed to increase of density of localized states in the conduction band.

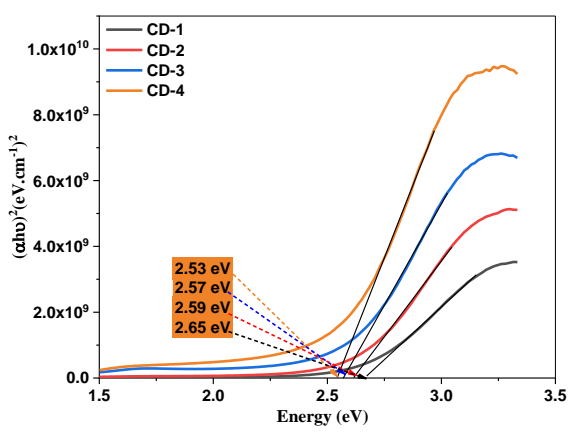


Fig. (7) Plots of $(\alpha h v)^2$ vs. (h v) for multilayer CdO thin films

The use of Hall measurements was applied in order to examine the impact of the number of layers on the concentration of charge carriers (n_H) and the Hall mobility (μ_H) in CdO films. The results indicated that there was a reduction in resistance as the number of layers grew, with the fifth layer demonstrating the lowest level of resistance. The aforementioned data are consistent with prior studies [29], which suggest a decrease in resistivity as the number of coatings increases, eventually reaching a minimum value for a certain number of layers. The increase in the number of layers leads to a higher concentration of charge carriers, which may be attributed to the increased availability of atoms and a decrease in scattering centers. Moreover, the existence of oxygen vacancies serves as a catalyst for augmenting conductivity, hence resulting in enhanced conductivity (i.e., a reduction in resistance) as the number of layers increases. The 5-layers sample exhibited the most advantageous result, with a maximum conductivity value of 0.753 (Ω .cm)⁻¹, as shown in table (2). This study offers further information on the produced films, including carrier concentration, mobility, and sample conductivity. The presented table illustrates

the augmentation of sample mobility with the progressive increment of deposited layers. The augmentation of μ_H has the potential to boost the gas sensitivity. A high charge carrier mobility is indicative of enhanced mobility of charge carriers inside the material, resulting in expedited reaction times and heightened sensor sensitivity. The electrical resistance of a sensor may be influenced by changes in the charge carrier mobility resulting from the interaction between a gas and the detecting material [30].

Table (2) Carrier concentration, mobility, and conductivity of prepared CdO films

Sample	n×10 ¹⁶ (cm ⁻³)	μ _H (cm²/V.s)	σ_{RT} $(\Omega^{-1}.cm^{-1})$	Туре
CD-1	-3.87	93	0.58	n-type
CD-2	-3.16	120	0.61	n-type
CD-3	-2.55	157	0.64	n-type
CD-4	-2.11	223	0.75	n-type

In order to improve the device sensitivity for a certain gas, the most appropriate operation temperature should be determined [31]. Taking into account that sensing reactions take place mainly at the sensor's surface layer, the control of semiconductor composition, morphology and microstructure is required for enhancing the sensitivity of the sensor. Working with nanostructured materials will give a larger surface. In gas sensor, the changing of resistance is just only influenced by the presence of amount of some gases of interest [32]. The sensitivity factor (*S*) calculation at different temperatures is determined using Eq. (4)

$$S = \frac{Rg - Ra}{Ra} \times 100\% \tag{4}$$

All four gas sensing samples (CD-1, CD-2, CD-3, and CD-4) deposited on glass substrates were tested as a function of operating temperatures (100, 200, and 300 °C) using reducing gas (H₂S) at a concentration of 125 ppm. Figure (8) presents the sensitivity of all four samples, with sample CD-4 (five layers) showing the most significant sensitivity from 72% to 125 ppm of H₂S at an operating temperature of 200 °C. This result is higher than that obtained by the researcher [33]. Samples CD-1, CD-2, and CD-3 also had high responses at 200 °C, 14%, 34%, and 38%, respectively. From the previous, for the sensor used for H₂S detection, the optimal sensitivity was obtained at 200 °C for the CD-4 sample and considered suitable sensitivity and medium temperature. The high sensitivity of sample CD-4 may be due to the large crystallite size, high roughness, and also high conductivity compared to other samples.

The sensitivity of gas sensors exhibits an increase with rising working temperatures, a phenomenon influenced by several factors tied to the surface properties of the sensing layer. An important consideration in this context is the type of gas being detected, whether it falls into the category of reducing

or non-reducing gases. The behavior of reducing gases at higher temperatures often involves chemical reactions that can modify the surface characteristics of the sensing layer, potentially leading to the formation of new layers that obstruct gas absorption and result in reduced sensitivity. Conversely, non-reducing gases tend to respond differently to elevated temperatures. These gases may experience increased molecular mobility and a higher rate of interaction with the sensing layer, initially boosting sensitivity. Therefore, when investigating the relationship between sensitivity and temperature, it is crucial to account for the specific gas type in question, as both reducing and non-reducing gases can exert distinct effects on sensitivity as temperature rises [34,35].

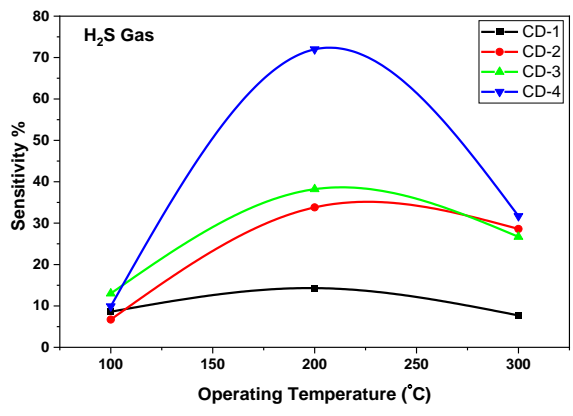


Fig. (8) Sensitivity of CdO thin films for H₂S gas

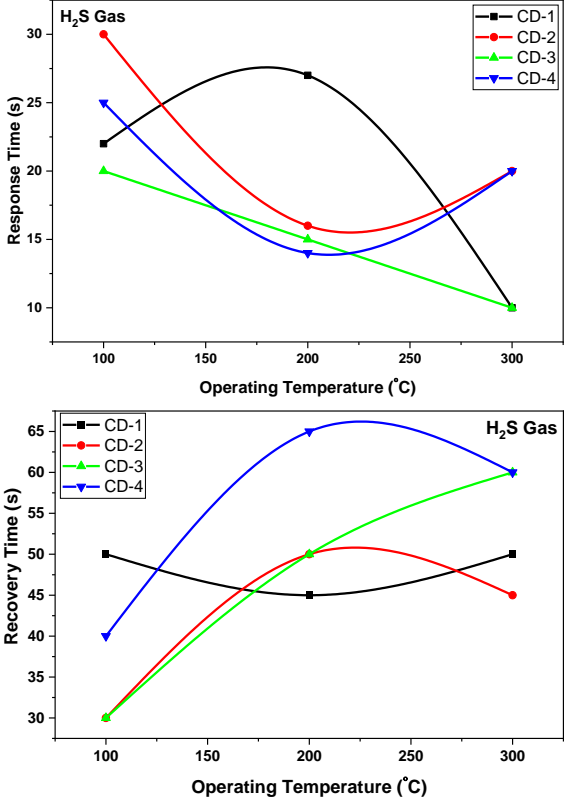


Fig. (9) Response and recovery times of CdO thin films used as gas sensors for H_2S gas

The increase in response with increase in temperature may be due to the supply of adequate thermal energy to overcome inter- granular barrier height. The decrease in response at higher temperature (300°C) is attributed to the excess thermal energy that may slow down the process of interaction with oxygen [33]. The relationship between response time and recovery time for CdO films with varying numbers of layers at different operating temperatures is depicted in Fig. (9). The deposition process was conducted on a glass substrate, employing an air mixing ratio of H₂S at 125 ppm. The graphical representation illustrates the rapid response rate (14 s) and the longest recovery time (65 s) exhibited by the cadmium oxide thin films comprising five layers, denoted as CD-4 at 200°C. The irregularities noted in the trend of response and recovery times for the CD-1 sample may be ascribed to surface irregularities evident in the AFM results.

4. Conclusion

This study has unveiled a clear connection between the thickness of the sensing layer (determined by the number of layers) and the porosity of the thin films. With an increase in the number of layers, the thin films exhibited higher porosity, accompanied by heightened surface roughness, enhanced conductivity, and larger grain sizes. The data on sensor performance have presented encouraging outcomes, particularly for the optimized sensing setup featuring five layers of CdO operating at a temperature of 200°C. This specific configuration showcased an impressive responsiveness of 72% in detecting H₂S gas. These findings underscore the importance of tailoring the thickness of CdO thin films to optimize their gas-sensing capabilities. The optimized configuration holds substantial promise for practical gas-sensing applications. This analysis serves as valuable guidance for the design and development of advanced gas sensors, aiming to achieve enhanced performance and heightened sensitivity.

References

- [1] A.S. Kamble et al., "Ethanol sensing properties of chemosynthesized CdO nanowires and nanowalls", *Mater. Lett.*, 65(10) (2011) 1488-1491.
- [2] A.A. Dakhel, "Structural, optical and electrical measurements on boron-doped CdO thin films", *J. Mater. Sci.*, 46 (2011) 6925-6931.
- [3] D.M. Carballeda-Galicia et al., "High transmittance CdO thin films obtained by the sol-gel method", *Thin Solid Films*, 371(1-2) (2000) 105-108.
- [4] W. Xia et al., "Investigation of CdO hexagonal nanoflakes synthesized by a hydrothermal method for liquefied petroleum gas detection", *Anal. Meth.*, 8(33) (2016) 6265-6269.

- [5] M. Ghosh and C.N.R. Rao, "Solvothermal synthesis of CdO and CuO nanocrystals", *Chem. Phys. Lett.*, 393(4-6) (2004) 493-497.
- [6] R.N. Bulakhe and C. D. Lokhande, "Chemically deposited cubic structured CdO thin films: use in liquefied petroleum gas sensor", *Sens. Actuat. B: Chem.*, 200 (2014) 245-250.
- [7] M. Yan et al., "Highly conductive epitaxial CdO thin films prepared by pulsed laser deposition", *Appl. Phys. Lett.*, 78(16) (2001) 2342-2344.
- [8] R.H. Bari and S.B. Patil, "Nanostructured CdO thin films for LPG and CO₂ gas sensor prepared by spray pyrolisis technique", *Int. Lett. Chem. Phys. Astron.*, 18 (2014) 31-46.
- [9] P. Dhivya, A.K. Prasad and M. Sridharan, "Magnetron sputtered nanostructured cadmium oxide films for ammonia sensing", *J. Solid State Chem.*, 214 (2014) 24-29.
- [10] B. Saha et al., "Quantum size effect on the optical properties of RF magnetron sputtered nanocrystalline cadmium oxide thin films", *Int. J. Nanosci.*, 10(4/5) (2011) 713-716.
- [11] I. Rathinamala, N. Jeyakumaran and N. Prithivikumaran, "Sol-gel assisted spin coated CdS/PS electrode based glucose biosensor", *Vacuum*, 161 (2019) 291-296.
- [12] M. Singh et al., "Synthesis and characterization of perovskite barium titanate thin film and its application as LPG sensor", *Sens. Actuat. B: Chem.*, 241 (2017) 1170-1178.
- [13] D. Pravarthana et al., "Highly sensitive and selective H₂S gas sensor based on TiO₂ thin films", *Appl. Surf. Sci.*, 549 (2021) 149281.
- [14] N. Barsan, M. Schweizer-Berberich and W. Göpel, "Fundamental and practical aspects in the design of nanoscaled SnO₂ gas sensors: a status report", *Fresenius' J. Anal. Chem.*, 365 (1999) 287-304.
- [15] A. Chapelle et al., "Structural and gas-sensing properties of CuO–Cu_xFe_{3-x}O₄ nanostructured thin films", *Sens. Actuat. B: Chem.*, 153(1) (2011) 117-124.
- [16] I. Ben Miled et al., "Influence of In-doping on microstructure, optical and electrical properties of sol–gel derived CdO thin films", *J. Mater. Sci.: Mater. in Electron.*, 29 (2018) 11286-11295.
- [17] S.A. Hameed et al., "Effect of thickness on structural and optical properties of cdo thin films prepared by chemical spray pyrolysis method", *NeuroQuantology*, 18(4) (2020) 20.
- [18] E.M. Nasir, "Thickness and gamma-ray effect on physical properties of CdO thin films grown by pulsed laser deposition", *Iraqi J. Phys.*, 14(29) (2016) 90-100.
- [19] B. Hymavathi, B.R. Kumar and T.S. Rao, "Effect of film thickness on physical properties of DC reactive magnetron sputtered Cr doped CdO thin fil", *J. Optoelectron. Adv. Mater.*, 17 (2015)

- 160-164.
- [20] M.A.R. Miranda and J.M. Sasaki, "The limit of application of the Scherrer equation", *Acta Crystallogr. A: Found. Adv.*, 74(1) (2018) 54-65
- [21] B. R. Kumar et al., "Enhancing the properties of CdO thin films by co-doping with Mn and Fe for photodetector applications", *Sens. Actuat. A: Phys.*, 319 (2021) 112544.
- [22] K. Usharani and A.R. Balu, "Structural, optical, and electrical properties of Zn-doped CdO thin films fabricated by a simplified spray pyrolysis technique", *Acta Metallurgica Sinica*, 28 (2015) 64-71.
- [23] M.H. Suhail, H.S. Al-Jumily and O.G. Abdullah, "Characterization and NO₂ gas sensing performance of CdO: In₂O₃ polycrystalline thin films prepared by spray pyrolysis technique", *SN Appl. Sci.*, 1 (2019) 1-12.
- [24] B. Gokul, P. Matheswaran and R. Sathyamoorthy, "Influence of annealing on physical properties of CdO thin films prepared by SILAR method", *J. Mater. Sci. Technol.*, 29(1) (2013) 17-21.
- [25] M. Althamthami et al., "Effect of different Cu:Co film concentrations on photocatalytic reactions of ethanol, MB, AMX, and Cr (VI): A study of film properties & effects of photooxidation", *J. Enviro. Chem. Eng.*, 11(6) (2023) 111247.
- [26] A.S. Hassanien and I.M. El Radaf, "Optical characterizations of quaternary Cu₂MnSnS₄thin films: novel synthesis process of film samples by spray pyrolysis technique", *Physica B: Cond. Matter*, 585 (2020) 412110.
- [27] H. Ullah, R. Rahaman and S. Mahmud, "Optical properties of cadmium oxide (CdO) thin films", *Indonesian J. Electr. Eng. Computer Sci.*, 5(1) (2017) 81-84.
- [28] M.H. Kabir et al., "Effect of annealing temperature on structural morphological and optical properties of spray pyrolized Al-doped ZnO thin films", *J. Phys. Commun.*, 3(10) (2019) 105007.
- [29] P. Sakthivel et al., "Improved optoelectronic properties of Gd doped cadmium oxide thin films through optimized film thickness for alternative TCO applications", *J. Alloys Comp.*, 820 (2020) 153188.
- [30] M.O. Salman, M.A. Kadhim and A.A. Khalefa, "CdO:SnO₂ Composite UV-Assisted Room Temperature Ozone Sensor", *Iraqi J. Sci.*, (2023) 1190-1202.
- [31] M.V. Nikolic et al., "Semiconductor gas sensors: Materials, technology, design, and application", *Sensors*, 20(22) (2020) 6694.
- [32] N.K. Abbas, I.M. Ibrahim and M.A. Saleh, "Characteristics of MEH-PPV/Si and MEH-PPV/PS heterojunctions as NO₂ gas sensors", *Silicon*, 10 (2018) 1345-1350.

- [33] C.R. Bobade et al., "Higher H₂S Gas Sensing Performance of Cadmium Zinc Mixed Oxide Thin Films Compared to Tin Doped and Pure Cadmium Oxide Thin Films Synthesized by Spray CVD Method", *phys. stat. sol.* (*a*), 177(2) (2000) 477-483.
- [34] C.R. Bobade, "Cadmium Oxide Thin Films Synthesized At Low Temperature By Spray
- CVD Technique for H₂S Gas Sensing Applications", *Int. J. Res. Biosci. Agric. Technol.*, 2 (2018) 118–125.
- [35] M. Kumar, A. Kumar and A.C. Abhyankar, "SnO₂ based sensors with improved sensitivity and response-recovery time", *Ceram. Int.*, 40(6) (2014) 8411-8418.

Table (1) XRD parameters for the CdO thin films prepared by Sol-gel technique at different numbers of layers

Sample	2θ (Deg.)	FWHM (Deg.)	d-space (Å)	Average D (nm)	Lattice constant a (Å)	hkl
,	33.0232	0.3590	2.7103	23.4	4.6902	(111)
CD-1	38.3827	0.3755	2.3433			(200)
	55.4107	0.4144	1.6568			(220)
,	33.0697	0.3013	2.7066	24.0	4.6909	(111)
CD-2	38.3251	0.3478	2.3467			(200)
CD-2	55.3107	0.4332	1.6596			(220)
	66.0075	0.4897	1.4142			(311)
	33.0320	0.2901	2.7096	25.2	4.6922	(111)
CD-3	38.3427	0.3225	2.3457			(200)
CD-3	55.3507	0.4143	1.6585			(220)
	65.9710	0.4708	1.4149			(311)
	33.0308	0.2430	2.7097	29.7	4.6928	(111)
	38.3427	0.2625	2.3457			(200)
CD-4	55.3096	0.3255	1.6596			(220)
	66.0015	0.3860	1.4143			(311)
	69.2644	0.4040	1.3554			(222)